

Federated Learning Assisted Deep Q-Learning for Joint Task Offloading and Fronthaul Segment Routing in Open RAN

Anselme Ndikumana, Kim Khoa Nguyen, *Senior Member, IEEE*,
and Mohamed Cheriet, *Senior Member, IEEE*,

Offloading computation-intensive tasks to edge clouds has become an efficient way to support resource constraint edge devices. However, task offloading delay is an issue largely due to the networks with limited capacities between edge clouds and edge devices. In this paper, we consider task offloading in Open Radio Access Network (O-RAN), which is a new 5G RAN architecture allowing Open Central Unit (O-CU) to be co-located with Open Distributed Unit (DU) at the edge cloud for low-latency services. O-RAN relies on fronthaul network to connect O-RAN Radio Units (O-RUs) and edge clouds that host O-DUs. Consequently, tasks are offloaded onto the edge clouds via wireless and fronthaul networks [1], which requires routing. Since edge clouds do not have the same available computation resources and tasks' computation deadlines are different, we need a task distribution approach to multiple edge clouds. Prior work has never addressed this joint problem of task offloading, fronthaul routing, and edge computing. To this end, using segment routing, O-RAN intelligent controllers, and multiple edge clouds, we formulate an optimization problem to minimize offloading, fronthaul routing, and computation delays in O-RAN. To determine the solution of this NP-hard problem, we use Deep Q-Learning assisted by federated learning with a reward function that reduces the Cost of Delay (CoD). The simulation results show that our solution maximizes the reward in minimizing CoD.

Index Terms—Task Offloading, Fronthaul Routing, Segment Routing, Edge Computing, Open Radio Access Network

I. INTRODUCTION

By the year 2025, there will be 34.2 billion edge devices, including 21.5 billion IoT devices [2]. Consequently, edge devices will be anywhere, anytime, and connected to anything. Therefore, it will be not only people who generate data but also machines/things [3]. However, edge devices have limited resources such as memory, CPU, and energy. Offloading computation-intensive tasks to edge clouds helps resource-constrained edge devices address this issue. However, networks between edge clouds and edge devices critically impact offloading delay.

To provide edge devices with low latency and high data rates, the 5G Radio Access Network (RAN) has experienced

Anselme Ndikumana, Kim Khoa Nguyen, and Mohamed Cheriet (Corresponding author) are with Synchronmedia Lab, École de Technologie Supérieure, Université du Québec, 1100 Notre-Dame St W, Montreal, QC H3C 1K3, Canada, (E-mail: anselme.ndikumana.1@ens.etsmtl.ca; kim-khoa.nguyen@etsmtl.ca; Mohamed.Cheriet@etsmtl.ca).

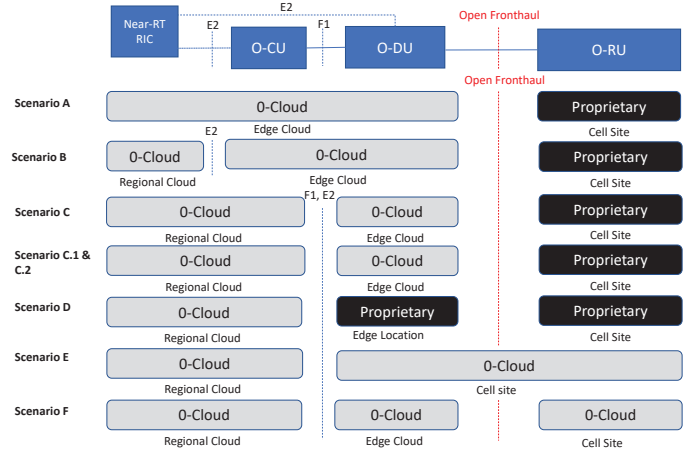


Figure 1: O-RAN deployment scenarios [4].

some transformations to increase deployment flexibility and network dynamics. The recent RAN transformation is Open Radio Access Network (O-RAN) architecture [5]. In O-RAN deployment scenarios shown in Fig. 1 and described in [4], O-DU and O-CU, where O stands for Open, can be modular base station software stacks on off-the-shelf server hardware that different vendors can supply. A low latency offloading service may require O-RAN deployment scenario A, where O-CU can be co-located with the O-DU at the edge cloud (e.g., a telecom room close to the edge devices). In scenario A, the edge cloud has O-Cloud that hosts O-RAN Central Unit Control Plane (O-CU-CP) and O-RAN Central Unit User Plane (O-CU-UP), O-DU, and Near-Real Time RAN Intelligent Controller (Near-RT RIC). Nearly real-time RAN resources and elements can be optimized using Machine Learning (ML) algorithms implemented in Near-RT RIC. Also, O-RAN has a Non-Real Time RAN Intelligent Controller (Non-RT RIC) that enables Machine Learning (ML) functionalities for policy-based guidance of applications and features. Using O-RAN, the tasks are offloaded onto the edge cloud via a wireless network between edge devices and O-RUs, and the fronthaul network linking O-RUs with the edge cloud that hosts O-DU [6]. Ideally, offloading should be based on a reliable fronthaul and wireless connection between edge devices and edge clouds. Unfortunately, it is not always the case in reality. Offloading traffic pressures and strict delay requirements for time-sensitive applications can significantly challenge wireless and fronthaul networks.

Currently, there are many fronthaul transport technologies described in [7] to reach edge clouds. Some of

these technologies are microwave, Passive Optical Network (PON), Wavelength-Division Multiplexing (WDM) PON, Coarse-WDM (CWDM) PON, Dense-WDM (DWDM), and Ethernet. Ethernet-based fronthaul network is a lower-cost solution that can reduce Capital Expenditure (CapEx) and Operating Expenses (OpEx) compared to other technologies [7]. Therefore, this paper considers Time-Sensitive Networking (TSN) [8] for Fronthaul as an Ethernet-based solution. IEEE 802.1CM [9] standard and Common Public Radio Interface (eCPRI) [10] allow to connect O-RUs to O-DUs using a packet network. Fronthaul traffic over the packet network enables switched connectivity between O-RUs and O-DUs. Therefore, we can route fronthaul traffic to edge clouds using multiple paths and hops. A class of low-latency 5G applications requires a fronthaul delay of 100 μ s for the user plane traffic [11]. To meet this requirement, we need a routing approach that simplifies the existing IP/Multi-Protocol Label Switching (MPLS) based strategies to reduce fronthaul latency. We consider Segment Routing (SR) [12] in the fronthaul network as a routing solution because it simplifies the control plane by removing the need for a per-flow state to be maintained at each node in MPLS. In other words, in SR, the per-flow state is only maintained at the ingress node of an SR domain. Still, there are many critical challenges for data offloading, fronthaul routing, and edge computing that have never been addressed in the literature, such as:

- The problem of task offloading, fronthaul routing, and edge computing should be addressed jointly to satisfy task computation deadlines.
- In forwarding decisions, TSN bridges for the fronthaul network use Ethernet header contents, not IP addresses. Therefore, we need a network approach that extends layer 2 as a network overlay for TSN fronthaul routing.
- When each edge cloud operates independently, required resources for offloaded computation-intensive tasks to the edge cloud may exceed available computation resources. Therefore, task distribution to multiple edge clouds should be considered.
- Computation tasks have different deadlines. Also, edge clouds do not have the same available computation resources. Therefore, we need a task distribution approach to multiple edge clouds to meet computation deadlines.

In this work, we opt for O-RAN and take advantage of O-RAN intelligent controllers to tackle the abovementioned challenges of task offloading, fronthaul routing, and edge computing. However, O-RAN is not restrictive; other RAT technologies considering the 7-2x split option (fronthaul between DU and RU can be applied). The main contributions of this paper are summarized as follows:

- We propose offloading approach for edge devices. The proposed approach enables edge devices with insufficient computation resources to balance the costs between keeping the computational task until the resources become available for local computation and offloading tasks to the edge cloud.
- We propose O-RAN fronthaul routing approach using

Near-RT RIC to route offloaded tasks to edge clouds. Since fronthaul TSN bridges use the Ethernet header contents, not the IP addresses, we consider Virtual Extensible LAN protocol (VXLAN) [13] to extend layer two connectivity as a network overlay. Then, we apply SR in the fronthaul network to route offloaded tasks to multiple edge clouds. To the best of our knowledge, this research is the first that leverages O-RAN controllers, SR, and VXLAN in a joint task offloading, fronthaul routing, and edge computing problem.

- We propose an edge cloud computing approach that enables edge cloud with insufficient resources to request computation support to its neighbor edge clouds or regional cloud through redirecting offloaded tasks.
- We formulate an optimization problem to minimize offloading, fronthaul routing, and computation delay. We convert the proposed NP-hard problem to the reward function for a dynamic offloading environment. Then, we design a Deep Q-Learning approach, assisted by federated learning, to maximize the reward function by reducing CoD.

As related work, task offloading in wireless networks [3], [14]–[17] has gained significant attention in research communities compared to offloading in fronthaul networks. Considering wireless and fronthaul networks between edge devices and edge clouds, the authors in [18] proposed an offloading approach in Cloud Radio Access Network (C-RAN), where the mobile device can change the offloading strategy to reduce fronthaul traffic. In [19] authors propose multi-hop fronthaul offloading in C-RAN and compare multi-hops with single-hop communication. For fronthaul routing, the authors in [20] proposed a lower latency scheme in C-RAN that enables the selection of a set of paths that minimizes delays from the preselected k shortest paths. The proposed C-RAN-based approaches consider fronthaul between Remote Radio Unit (RRU) and Baseband Processing Unit (BBU). However, we have fronthaul between O-RUs and O-DUs and middlehaul between DUs and CUs in O-RAN. Since our proposal considers O-DU and O-CU to be hosted at the same edge cloud in O-RAN, the middlehaul network is outside this paper’s scope. To apply machine learning in data offloading, the authors in [21] highlight that exchanging raw data may slow down wireless communication services. Therefore, the authors in [22] emphasized that sharing only machine learning parameters of federated learning without sharing raw data can be an appropriate solution to address this issue. The authors in [23] proposed intelligent task offloading approach that uses a federated Q-learning method to minimize the probabilities of data offloading failure by considering communication and computing budgets. However, the authors did not consider fronthaul network in offloading data to the edge cloud. In [24], the authors applied a deep Monte Carlo tree search in data offloading. Their proposed approach enables an agent to observe the network environment and decide the offloading actions. To address the issue of limited resource sharing in data offloading, the authors in [25] formulated a computation offloading problem using a multi-agent Markov

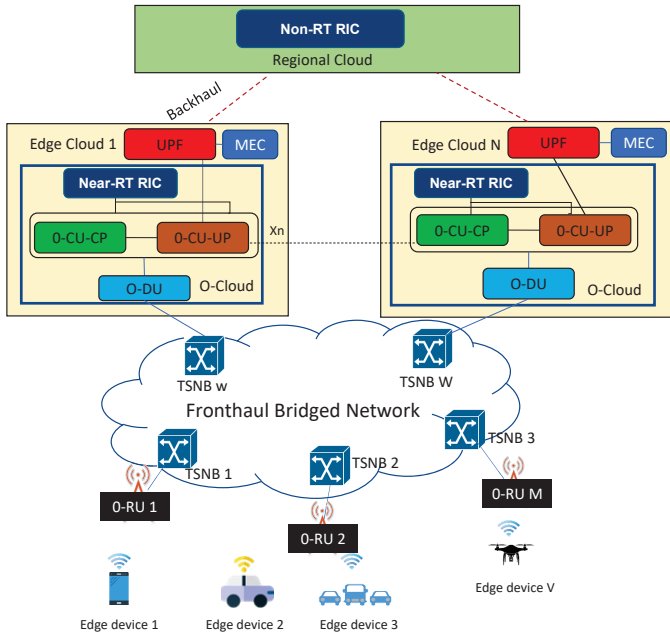


Figure 2: Illustration of our system model.

decision process in multi-access edge computing. However, the previous related works have never addressed the issue of joint task offloading, fronthaul routing, and edge computing.

The rest of this paper is structured as follows: we present our system model in Section II, while Section III describes in detail our task offloading, fronthaul routing, and cloud computation. We present our problem formulation and solution in Section IV. Section V presents our performance evaluation. We conclude the paper in Section VI.

II. SYSTEM MODEL

The system model of our joint task offloading, fronthaul routing, and cloud computation approach is depicted in Fig. 2. For easy visualization of the system model, we omit some interfaces in Fig. 2.

In the system model, we consider \mathcal{V} as a set of edge devices. Each edge device $v \in \mathcal{V}$ has computation-intensive tasks that need to use computation resources, such as on-device machine learning and Extended Reality (it combines Virtual Reality and Augmented Reality [26]). For example, in XR, edge devices participating in crowd-sensing [27] can sense their environment, compute sensed data, and create virtual environment. However, if the edge device does not have resources, it can send tasks and data to the edge cloud for computation and creating the virtual environment. We define a task $\Gamma_v = (d_v, \tilde{\tau}_v, \tilde{z}_v)$, where d_v is the size of computation input data from edge device v in terms of bits, $\tilde{\tau}_v$ is the task computation deadline, and \tilde{z}_v is the computation workload or intensity in terms of CPU cycles per bit. Each edge device $v \in \mathcal{V}$ has computation capability χ_v . Offloading happens when the edge device does not have enough computation resources, and it can not hold computational tasks until the resource becomes available.

Table I: Summary of key notations.

Notation	Definition
\mathcal{N}	Set of Edge Clouds (ECs), $ \mathcal{N} = N$
\mathcal{M}	Set of O-RUs, $ \mathcal{M} = M$
\mathcal{V}	Set of edge devices, $ \mathcal{V} = V$
\mathcal{W}	Set of fronthaul TSNBs, $ \mathcal{W} = W$
Γ_v	Computation task of edge device $v \in \mathcal{V}$
τ_v^{loc}	Local computational delay of device v
τ_v^{off}	Offloading delay of device v
μ_v	Status parameter of device v
\mathcal{E}	Set of fronthaul links, $ \mathcal{E} = E$
χ_n	Computation capability of EC $n \in \mathcal{N}$
χ_v	Computation resource of device $v \in \mathcal{V}$
$x_v^{m \rightarrow n}$	Offloading variable of device $v \in \mathcal{V}$
ω_v^m	Wireless capacity between device v and EC m
ω_i^j	Fronthaul capacity of link $e_{i,j}$
ω_n^q	Link capacity between EC n and EC q
ω_n^{RC}	Backhaul capacity between EC n and RC
\mathcal{R}	Reward
\mathcal{A}	Action space
\mathcal{S}	State space
\mathcal{P}	Transition probability matrix

Task offloading requires communication resources. Therefore, each edge device $v \in \mathcal{V}$ is connected to O-RU $m \in \mathcal{M}$ via a wireless link of capacity ω_v^m . Here, we denote \mathcal{M} as a set of O-RUs. Once offloaded tasks reach O-RUs, the O-RUs forward the task to O-DUs using Fronthaul Bridged Network (FBN) of multiple paths. We model FBN as graph $\mathcal{G} = (\mathcal{W}, \mathcal{E})$, where \mathcal{W} is the set of Time-Sensitive Networking Bridges (TSNBs) and \mathcal{E} is the set of links. In FBN, each O-RU m is connected to ingress TSNB, and each O-DU is connected to egress TSNB. We denote \mathcal{N} as a set of Edge Clouds (ECs) that host O-DUs. We use the terms ‘‘EC’’ and ‘‘O-DU’’ interchangeably. O-DU $n \in \mathcal{N}$ means the O-DU hosted at EC n . To route offloaded tasks using multiple paths, we use SR in FBN, where Near-RT RIC at EC controls fronthaul SR. To implement SR described in Section III-C, we assume that VXLAN is applied in FBN. We choose VXLAN [13] over Virtual LAN (VLAN) because VXLAN uses a VXLAN network identifier of 24 bits, while VLAN has a network identifier of 12 bits. Therefore, VLAN can be scaled up to 4000 VLANs, while VXLAN can be scaled up to 16 million VXLANs segments. Combining SR and VXLAN can help the network to handle massive fronthaul traffic offloading that needs to be routed to multiple ECs. In implementing SR using VXLAN, we assume Near-RT RIC knows the FBN topology and can communicate with all TSNBs. The Near-RT RIC records traffic matrix. With the MEC server’s help, traffic matrix, and network topology information, the Near-RT RIC has the segment paths for each source-destination pair in the FBN.

Each EC has an MEC server, User Plane Function (UPF), and O-Cloud to improve reliability and lower latency in data offloading. Once the tasks reach O-DU via egress TSNB,

the O-DU sends them to the MEC server accessible via O-CU-UP and UPF for computation. Each MEC $n \in \mathcal{N}$ has a computational resource of capacity χ_n that can be allocated to edge devices. Here, unless stated otherwise, we use the terms ‘‘EC’’ and ‘‘MEC’’ interchangeably. MEC $n \in \mathcal{N}$ means the MEC hosted at EC n . Here, we assume ECs can exchange application-level data using Xn interface [28]. Furthermore, each EC $n \in \mathcal{N}$ has access to the Regional Cloud (RC) via a wired backhaul of capacity ω_n^{RC} . When computation resources are unavailable in ECs, the tasks will be offloaded to the RC in the worst-case scenario. We denote χ_{RC} as the computation capacity of the RC. Each RC hosts Non-RT RIC. Unless stated otherwise, we use the terms ‘‘RC’’, and ‘‘Non-RT RIC’’ interchangeably.

III. TASK OFFLOADING, FRONTHAUL ROUTING, AND CLOUD COMPUTATION

This section discusses our task offloading approach that enables edge devices to balance the costs of local computation and offloading tasks to the edge cloud. Furthermore, we present the models for wireless communication and fronthaul routing that enable offloaded tasks to reach edge clouds. We conclude the section with a computation model for edge and regional clouds.

A. Computation at Edge Devices

Each edge device $v \in \mathcal{V}$ has an application that generates computation task Γ_v . Computing task Γ_v at edge device v requires CPU computation resources. By using computation resource χ_v , the execution latency for task Γ_v at edge device v is given by:

$$\tau_v = \frac{d_v \tilde{z}_v}{\chi_v}. \quad (1)$$

When $\tau_v > \tilde{\tau}_v$, or $\tilde{z}_v > \chi_v$, edge device v does not have enough resources or cannot meet the computation deadline. Therefore, the edge device can hold on the computational task until the resources become available for local computation or offload the task to the edge cloud. To handle such a situation, we define the edge device status parameter $\mu_v \in \{0, 1\}$, where μ_v is expressed as follows:

$$\mu_v = \begin{cases} 0, & \text{if } \tau_v > \tilde{\tau}_v, \text{ or } \tilde{z}_v > \chi_v, \\ 1, & \text{otherwise.} \end{cases} \quad (2)$$

Based on $\mu_v \in \{0, 1\}$, the total local execution time τ_v^{loc} of task Γ_v at edge device v becomes:

$$\tau_v^{\text{loc}} = \begin{cases} \tau_v, & \text{if } \mu_v = 1, \text{ and } x_v^{m \rightarrow n} = 0, \\ \tau_v + \varphi_v, & \text{if } \mu_v = 0, \text{ and } x_v^{m \rightarrow n} = 0, \\ 0, & \text{if } \mu_v = 0 \text{ and } x_v^{m \rightarrow n} = 1, \end{cases} \quad (3)$$

where φ_v is the average hold time for task Γ_v until it is locally computed at edge device v . The φ_v can be considered as a time for charging the battery or finishing ongoing computation of other tasks than Γ_v . When edge device v cannot hold on computational task, it can offload task to

the edge cloud. Therefore, we define $x_v^{m \rightarrow n} \in \{0, 1\}$ as an offloading decision variable, where $x_v^{m \rightarrow n}$ is given by:

$$x_v^{m \rightarrow n} = \begin{cases} 1, & \text{if } \Gamma_v \text{ is offloaded from edge device } v \text{ to} \\ & \text{EC } n \text{ via O-RU } m \\ 0, & \text{otherwise.} \end{cases} \quad (4)$$

B. Task Offloading in Wireless Networks

Offloading a task from the edge device $v \in \mathcal{V}$ to EC $n \in \mathcal{N}$ via O-RU $m \in \mathcal{M}$ requires wireless communication between each edge device v and O-RU m . The spectrum efficiency (as described in [29]) for edge device v is given by:

$$\gamma_v^m = \log_2 \left(1 + \frac{\rho_v |G_v^m|^2}{\sigma_v^2} \right), \quad \forall v \in \mathcal{V}, m \in \mathcal{M}. \quad (5)$$

Here, ρ_v is the transmission power of edge device, $|G_v^m|^2$ is the channel gain between edge device v and O-RU m , and σ_v^2 is the power of the Gaussian noise at edge device v . The instantaneous data rate for edge device v is expressed as:

$$B_v^m = x_v^{m \rightarrow n} b_v^m \omega_v^m \gamma_v^m, \quad \forall v \in \mathcal{V}, m \in \mathcal{M}, \quad (6)$$

where each edge device v is allocated a fraction b_v^m ($0 \leq b_v^m \leq 1$) of bandwidth ω_v^m . We assume that the spectrum of the mobile network operator is orthogonal, and there is no interference among the edge devices. Furthermore, we assume that the demand of edge devices for task offloading will only be accepted if there are enough spectrum resources to satisfy its demand. Based on the instantaneous data rate, the transmission delay for offloading a task from edge device v to EC n is expressed as:

$$\tau^{v \rightarrow m} = x_v^{m \rightarrow n} \frac{d_v}{B_v^m}, \quad \forall v \in \mathcal{V}, m \in \mathcal{M}. \quad (7)$$

C. Task Offloading in Fronthaul Bridged Network

When the offloaded tasks reach O-RUs, the O-RUs forward them to O-DUs using FBN. Since O-DUs are hosted at ECs, the offloaded tasks can reach ECs using multiple fronthaul paths. To route the offloaded tasks to O-DU, we use SR described below.

1) Overview of Segment Routing

The existing fronthaul routing in [20] is based on the shortest path algorithm in C-RAN. Here, we use SR [12] in O-RAN as a source routing approach because it overcomes the MPLS Traffic-Engineering (MPLS-TE) per-flow state that needs to be maintained in each network node to support traffic-engineered paths in IP backbones. SR improves MPLS-TE in labeling, where SR does not require configuring forwarding tables in each node along the transmission path. SR includes the route in the packet header at the ingress node. In other words, SR adds a list of hops in the packet header as a route.

As an illustrative example, we consider SR in Fig. 3, where the SR domain is defined as a set of TSNBs participating in the source-based routing model. In other words, O-RUs and O-DUs are connected to the segment domain but not

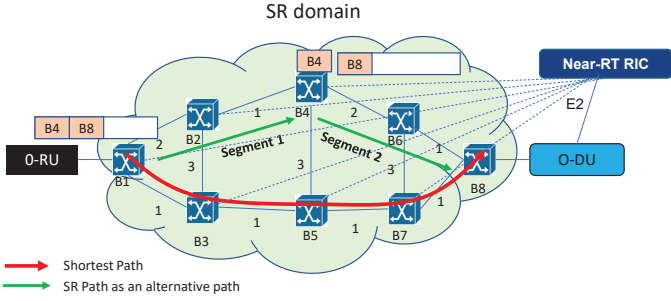


Figure 3: Illustration example of segment routing in FBN.

included in the SR domain. Since we use VXLAN, we can have multiple fronthaul segment domains over one physical FBN, where each Near-RT RIC controls one domain. The ingress TSNB $B1$ adds the segment label $B4$ and $B8$ to the packet header, where $B8$ is the destination address. The packet is routed from $B1$ to $B4$ along the shortest path $B1 - B2 - B4$. The top label is popped at bridge $B4$, and the packet is routed to $B8$. In other words, we have two segments, $B1 - B2 - B4$ and $B4 - B6 - B8$. Routing within each segment is done by the Interior Gateway Protocol (IGP) routing protocol such as Open Shortest Path First (OSPF). In other words, each link is associated with cost, and IGP can use the cost to choose the shortest path. The path (red path) from source to destination can be the shortest, but it does not guarantee to be the fastest route. Also, the shortest path may fail. Therefore, we consider the SR path (green path) as the best way to choose an alternative path based on the network delay.

2) Segment Routing in Fronthaul Network

We assume that ECs are close to the edge devices. Therefore, we use two segments in SR for FBN. As highlighted in [30], SR with two segments is generally enough in traffic planning problems that aim to route traffic so that no link is overloaded. However, extending from two segments to multiple segments is straightforward.

In our SR, Near-RT RIC chooses intermediate TSNB $w \in \mathcal{W}$ that splits the fronthaul path into two segments. Let us consider $i \in \mathcal{W}$ as source TSNB and $j \in \mathcal{W}$ as destination TSNB. When $w \neq i$ and $w \neq j$, the offloaded traffic is first routed on the shortest path $\Psi_{i,w}$ from i to w and then on the shortest path $\Psi_{w,j}$ from w to j . To route the offloaded traffic via FBN, the amount of traffic from i to j through intermediate TSNB w is given by:

$$l_{i,j}^w = \sum_{\mathcal{V}_{i,j}^w \subset \mathcal{V}} x_v^{m \rightarrow n} d_v, \quad (8)$$

where $\mathcal{V}_{i,j}^w \subset \mathcal{V}$ is a set of edge devices using fronthaul path $\Psi_{i,j}^w = \Psi_{i,w} \cup \Psi_{w,j}$ from i to j through intermediate TSNB w . The important node w as middle point for traffic routing can be chosen based on node centrality approach presented in [31]. We use $\tau_{SR}^{v,m \rightarrow n}$ as transmission delay of each fronthaul link using SR, where $\tau_{SR}^{v,m \rightarrow n}$ is given by:

$$\tau_{SR}^{v,m \rightarrow n} = \frac{l_{i,j}^w}{\omega_j^i}. \quad (9)$$

However, when the fronthaul network is not segmented,

the offloaded traffic is routed using a shortest path $\Psi_{i,j}$. Transmission delay $\tau_{SP}^{v,m \rightarrow n}$ for shortest path becomes $\tau_{SP}^{v,m \rightarrow n} = \frac{l_{i,j}}{\omega_j^i}$, where $l_{i,j} = \sum_{\mathcal{V}_{i,j} \subset \mathcal{V}} x_v^{m \rightarrow n} d_v$. Here, $\mathcal{V}_{i,j} \subset \mathcal{V}$ is a set of edge devices using fronthaul shortest path $\Psi_{i,j}$ from i to j .

Considering the shortest path $\Psi_{i,j}$ and the SR path $\Psi_{i,j}^w$, the Near-RT RIC needs to choose one path that gives the lowest possible latency to reach egress node. Therefore, we define fronthaul path selection variables, where $\eta_{SP}^{m \rightarrow n}$ is for SP and $\eta_{SR}^{m \rightarrow n}$ is for the SR, such that $\eta_{SP}^{m \rightarrow n} + \eta_{SR}^{m \rightarrow n} = 1$.

$$\eta_{SP}^{m \rightarrow n} = \begin{cases} 1, & \text{if } \tau_{SP}^{v,m \rightarrow n} \leq \tau_{SR}^{v,m \rightarrow n}, \\ 0, & \text{otherwise,} \end{cases} \quad (10)$$

$$\eta_{SR}^{m \rightarrow n} = 1 - \eta_{SP}^{m \rightarrow n} \quad (11)$$

If the shortest route has more transmission delay than the SR path, the ingress TSNB uses the SR path. Therefore, the fronthaul transmission delay becomes:

$$\tau_v^{m \rightarrow n} = \eta_{SP}^{m \rightarrow n} \tau_{SP}^{v,m \rightarrow n} + \tau_{SR}^{v,m \rightarrow n} \eta_{SR}^{m \rightarrow n}. \quad (12)$$

D. Computation at Edge and Regional Clouds

1) Computation at Edge Clouds

Once tasks reaches O-DU, the O-DU sends it to MEC server r via O-CU-UP and UPF. Then, MEC server checks if it has computation resource χ_{vn} required to compute task Γ_v from edge device v . The χ_{vn} can be computed as follows:

$$\chi_{vn} = \chi_n \frac{\tilde{z}_v}{\sum_{g \in \mathcal{V}_n} \tilde{z}_g}, \quad \forall v \in \mathcal{V}_n, n \in \mathcal{N}, \quad (13)$$

where \mathcal{V}_n is a set of edge devices connected to EC n . In Eq. (13), we use weighted proportional allocation, which is available in systems such as 4G and 5G cellular networks for resource allocation [32].

If $\chi_n - \chi_{vn} \leq \Theta_n$, the EC n allocates χ_{vn} to the task Γ_v . Here, Θ_n is resource allocation threshold of EC n . Furthermore, we define $y_v^{m \rightarrow n}$ as a computation decision variable, where $y_v^{m \rightarrow n}$ is given by:

$$y_v^{m \rightarrow n} = \begin{cases} 1, & \text{if } \Gamma_v \text{ offloaded via O-RU } m \\ & \text{is computed at EC } n (\chi_n - \chi_{vn} \leq \Theta_n), \\ 0, & \text{otherwise.} \end{cases} \quad (14)$$

The total computation resource allocations must satisfy:

$$\sum_{v \in \mathcal{V}_n} x_v^{m \rightarrow n} \chi_{vn} y_v^{m \rightarrow n} \leq \chi_n, \quad \forall n \in \mathcal{N}. \quad (15)$$

Using the computation resource χ_{vn} , the execution latency τ_{vn} of task Γ_v from edge device v at EC n becomes:

$$\tau_{vn} = \frac{d_v \tilde{z}_v}{\chi_{vn}}. \quad (16)$$

Furthermore, the total execution and offloading time for task Γ_v at EC n is given by:

$$\tau_{vn}^e = \tau^{v \rightarrow m} + \tau_v^{m \rightarrow n} + \tau_{vn}. \quad (17)$$

When $\chi_n - \chi_{vn} > \Theta_n$ or $\tilde{z}_v > \tau_{vn}^e$ or $\tau_{vn} > \tilde{\tau}_v$, we consider EC n to be overloaded. EC n requests support to

any neighboring EC q that has enough resources to satisfy the offloading demand and is located in less distance than RC by redirecting a task with high computation deadline. Otherwise, EC n requests support RC. As proposed in [3], we assume that ECs exchange the resource utilization information. The EC n checks resource utilization information of neighboring ECs, then compares EC q that has enough resources with RC using propagation delay. We use $\tau^{n \rightarrow q}$ to denote propagation delay between EC q and EC n , where $\tau^{n \rightarrow q}$ can be expressed as follows:

$$\tau^{n \rightarrow q} = \frac{L^{n \rightarrow q}}{\kappa}, \quad \forall r, q \in \mathcal{R}, \quad (18)$$

where $L^{n \rightarrow q}$ is the length of physical link between EC q and EC n and κ is the propagation speed. Furthermore, the propagation delay $\tau^{n \rightarrow RC}$ between EC n and RC can be expressed as follows:

$$\tau^{n \rightarrow RC} = \frac{L^{n \rightarrow RC}}{\kappa}, \quad \forall n \in \mathcal{N}, \quad (19)$$

where $L^{n \rightarrow RC}$ is the length of physical link between EC n and RC. We define a task forwarding decision variable $x_v^{n \rightarrow q}$, which indicates whether or not the task of edge device v is forwarded from EC n to EC q for computation. $x_v^{n \rightarrow q}$ is given by:

$$x_v^{n \rightarrow q} = \begin{cases} 1, & \text{if } \tau^{n \rightarrow q} \leq \tau^{n \rightarrow RC}, \\ 0, & \text{otherwise.} \end{cases} \quad (20)$$

The execution latency τ_{vq} of task Γ_v at EC q can be calculated using a similar approach as in (16). Therefore, the total execution time for a task offloaded by edge device v to EC q becomes:

$$\tau_{vnq}^e = \tau^{v \rightarrow m} + \tau_v^{m \rightarrow n} + \tau_v^{n \rightarrow q} + \tau^{n \rightarrow q} + \tau_{vq}. \quad (21)$$

Furthermore, the offloading delay $\tau_v^{n \rightarrow q}$ between EC n and EC q can be calculated as follows:

$$\tau_v^{n \rightarrow q} = \frac{\sum_{v \in \mathcal{V}_n} x_v^{n \rightarrow q} d_v}{\omega_n^q}, \quad \forall r, q \in \mathcal{R}, \quad (22)$$

where ω_n^q is link capacity between EC n and EC q .

2) Offloading Tasks to the Regional Cloud

When there are no available computation resources at any neighboring EC q , or EC q is at far distance than RC, the EC n forwards the task to the RC. Therefore, we define $x_v^{n \rightarrow RC}$ as offloading decision variable that indicates whether or not the task of edge device v is offloaded by EC n to the RC:

$$x_v^{n \rightarrow RC} = \begin{cases} 1, & \text{if } \tau^{n \rightarrow q} > \tau^{n \rightarrow RC} \text{ or no available resources} \\ & \text{at ECs,} \\ 0, & \text{otherwise.} \end{cases} \quad (23)$$

We define $\tau_v^{n \rightarrow RC}$ as the offloading delay between EC n and RC, where $\tau_v^{n \rightarrow RC}$ is given by:

$$\tau_v^{n \rightarrow RC} = \frac{\sum_{v \in \mathcal{V}_n} x_v^{n \rightarrow RC} d_v}{\omega_n^{RC}}, \quad \forall n, q \in \mathcal{N}. \quad (24)$$

ω_n^{RC} is the link capacity between EC n and RC. Therefore, the total execution time for task Γ_v offloaded by edge device v at RC becomes:

$$\tau_{vnRC}^e = \tau^{v \rightarrow m} + \tau_v^{m \rightarrow n} + \tau_v^{n \rightarrow RC} + \tau^{n \rightarrow RC} + \tau_{vRC}, \quad (25)$$

where τ_{vRC} can be calculated using a similar approach as in (16).

The total offloading and computation latency τ_v^{off} of task Γ_v from edge device v is given by:

$$\tau_v^{\text{off}} = y_v^{m \rightarrow n} \tau_{vn}^e + (1 - y_v^{m \rightarrow n})(x_v^{n \rightarrow q} \tau_{vnq}^e + x_v^{n \rightarrow RC} \tau_{vnRC}^e). \quad (26)$$

To ensure that task Γ_v from edge device v is executed at only one location, i.e., computed locally at a edge device, or at one of ECs, or at RC, we impose the following constraints:

$$(1 - x_v^{m \rightarrow n}) + x_v^{m \rightarrow n}(y_v^{m \rightarrow n} + n_v^{\text{sup}}) = 1, \quad (27)$$

where $n_v^{\text{sup}} = 1 - y_v^{m \rightarrow n}(x_v^{n \rightarrow q} + x_v^{n \rightarrow RC})$ corresponds to the support EC n gets from neighboring EC q or RC to compute the offloaded task Γ_v .

IV. PROBLEM FORMULATION AND SOLUTION

This section discusses the problem formulation for minimizing total delay, including offloading, fronthaul routing, and computation delays. Then, we present the solution approach of the formulated problem.

A. Problem Formulation

Computing task Γ_v locally at the edge device v requires computational delay cost τ_v^{loc} . On the other hand, computing offloaded task Γ_v at the EC or RC requires offloading, fronthaul routing, and cloud computation delays τ_v^{off} . We assume that the offloading decision making operates in time frames $t \in \mathcal{T} = \{1, 2, \dots, T\}$. Therefore, considering both local computation and offloading at time t , we formulate the following optimization problem to minimize total delay.

$$\min_{\mathbf{x}, \boldsymbol{\eta}, \mathbf{y}} \sum_{n \in \mathcal{N}} \sum_{v \in \mathcal{V}_n} (1 - x_v^{m \rightarrow n}(t)) \tau_v^{\text{loc}}(t) + x_v^{m \rightarrow n}(t) \tau_v^{\text{off}}(t) \quad (28)$$

subject to

$$\sum_{v \in \mathcal{V}_n} x_v^{m \rightarrow n}(t) b_v^m(t) \leq 1, \quad \forall m \in \mathcal{M}, \quad (28a)$$

$$x_v^{m \rightarrow n}(t) (\eta_{SP}^{m \rightarrow n}(t) l_{i,j}(t) + \eta_{SR}^{m \rightarrow n}(t) l_{i,j}^w(t)) \leq \omega_i^j(t), \quad (28b)$$

$$\sum_{v \in \mathcal{V}_n} x_v^{m \rightarrow n}(t) \chi_{vn}(t) y_v^{m \rightarrow n}(t) \leq \chi_n(t), \quad \forall n \in \mathcal{N}. \quad (28c)$$

The objective function in (28) combines (3), (26), and (27). The constraint in (28a) guarantees that the sum of wireless resources allocated to all edge devices has to be less than or equal to the total available resources. The constraint in (28b) is related to FBN, ensuring that each TSNB does not send more traffic than the link capacity. The constraint in (28c) guarantees that the computation resources allocated to edge devices at each EC do not exceed available computation resources.

The problem in (28) is combinatorial optimization problem, which is NP-hard. Also, using combinatorial optimization, the number of possibilities increases exponentially as the problem size increases. However, a heuristic approach can be designed to solve it. As an example, by applying Block Successive Majorization Minimization (BSMM) technique described in [33], [34], we can get a proximal convex surrogate problem by adding the quadratic term to (28) and relaxing variables. Then, we can minimize the proximal convex surrogate problem. However, the heuristic approach may results in a stationary solution, which is not appropriate for a dynamic environment. Therefore, we change the problem in (28) to be a reward function r_t which can be maximized by an existing ML approach such Deep Reinforcement Learning (DRL) [35]. Also, r_t can represent network condition:

$$\begin{aligned}
r_t = & \varpi_{\text{CoD}} \left(\sum_{n \in \mathcal{N}} \sum_{v \in \mathcal{V}_n} \tilde{\tau}_v(t) - ((1 - x_v^{m \rightarrow n}(t)) \tau_v^{\text{loc}}(t) + \right. \\
& \left. x_v^{m \rightarrow n}(t) \tau_v^{\text{off}}(t)) + \varpi_w \left(1 - \sum_{v \in \mathcal{V}_n} x_v^{m \rightarrow n}(t) b_v^m(t) \right) + \right. \\
& \left. \varpi_f (\omega_i^j(t) - x_v^{m \rightarrow n}(t) (\eta_{SP}^{m \rightarrow n}(t) l_{i,j}(t) + \eta_{SR}^{m \rightarrow n}(t) l_{i,j}^w(t))) + \right. \\
& \left. \varpi_c (\chi_n(t) - \sum_{v \in \mathcal{V}_n} x_v^{m \rightarrow n}(t) \chi_{vn}(t) y_v^{m \rightarrow n}(t)). \quad (29)
\end{aligned}$$

In the reward function (29), ϖ_{CoD} is the Cost of Delay (CoD), which represents the penalty for missing the computation deadline $\tilde{\tau}_v(t)$ in offloading. Similarly, we use ϖ_w to denote the penalty of violating wireless communication resource constraint, and ϖ_f is the penalty for overloading the fronthaul link capacity. ϖ_c is the penalty for violating computational resources constraint. The penalties ϖ_{CoD} , ϖ_c , ϖ_f , and ϖ_c correspond to the constraints in (28a), (28b), and (28c), respectively. In other words, using penalties, r_t goes down (Figs 11 and 12) when any of these constraints is violated.

B. Proposed Solution

One of the emerging approaches for handling (29) is to use ML algorithms such as DRL. In DRL, a DRL agent acts in the environment to find a proximal solution for a given problem. DRL considers time-varying workloads and network conditions, where the Markov Decision Process (MDP) can be applied to model the environment (detailed procedures of MDP are defined in [36]). In our solution approach presented in Fig. 4, we consider tuple $\langle \mathcal{A}, \mathcal{S}, \mathcal{R}, \mathcal{P} \rangle$ defined as follows:

- We consider the action space $\mathcal{A} = \{(\mathbf{x}, \mathbf{b}, \boldsymbol{\eta}, \mathbf{y})\}$ that represents the offloading decisions, communication resource allocation and routing decisions, and computation resources allocation decision.
- We define a state space \mathcal{S} which consists of current local computation, offloading using wireless and fronthaul, and cloud computation states such that $\mathcal{S} = \{(\boldsymbol{\tau}^{\text{loc}}, \boldsymbol{\tau}^{\text{off}}, \boldsymbol{\omega}, \mathbf{l}, \boldsymbol{\chi})\}$.
- We represent $\mathcal{R} = \sum_{t \in \mathcal{T}} r_t$ as an accumulated reward which indicates how action chosen in particular state improves resource allocation and CoD;

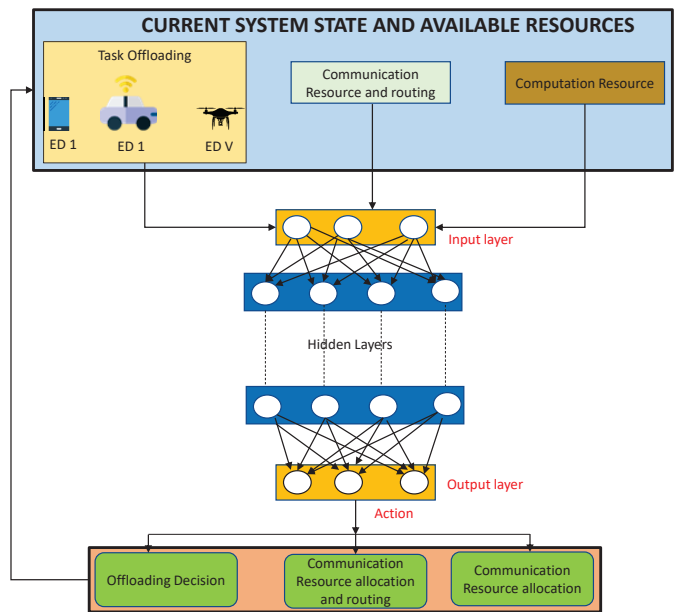


Figure 4: DRL process to solve (29).

- We use $\mathcal{P} = \{p(s_{t+1}, r_t | s_t, a_t)\}$ as the transition probability matrix that governs transition dynamics from one state $s_t \in \mathcal{S}$ to another $s_{t+1} \in \mathcal{S}$ in response to action $a_t \in \mathcal{A}$ and reward $r_t \in \mathcal{R}$.

The state transition and reward are stochastic and modeled as an MDP. The state transition probabilities and rewards depend only on the state of the offloading environment and the agent's action. The transition from $s_t \in \mathcal{S}$ to $s_{t+1} \in \mathcal{S}$ with reward $r_t \in \mathcal{R}$ when action $a_t \in \mathcal{A}$ chosen is characterized by the conditional transition probability \mathcal{P} , which is only determined by offloading environment.

In Fig. 4 (ED means edge device), the MEC server as an agent periodically learns to take actions, observes the most reward, and automatically adjusts its strategy. In DRL, we use Deep Q-Learning (DQL) [37]. We consider DQL as a better solution that leverages deep neural networks (DNNs) to train the deep learning model. In other words, DQL integrates deep learning into Q-Learning. The simplest form of Q-Learning, which is called one-step Q-Learning, is given by:

$$Q(s_t, a_t) = Q(s_t, a_t) + \alpha [r_{t+1} + \Upsilon Q(s_{t+1}, a) - Q(s_t, a_t)], \quad (30)$$

where α is the learning rate and $a \in \mathcal{A}$ is an action that was taken in the state s_t by the agent. Υ ($0 < \Upsilon \leq 1$) is discount factor that encourages the agent to account more for short-term reward r_t . On the other hand, DQL uses standard feed-forward neural networks to calculate Q-Value. The DQL uses two networks, Q-Network to calculate Q-Value in the state S_t and target network to calculate Q-Value in the state $S_t + 1$ such that:

$$Q(s_t, a_t) = Q(s_t, a_t) + \alpha [r_{t+1} + \Upsilon \max_a Q(s_{t+1}, a) - Q(s_t, a_t)]. \quad (31)$$

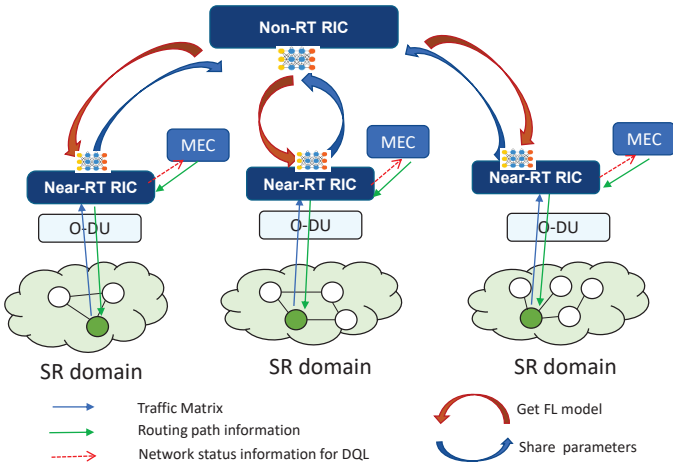


Figure 5: FL assisted DQL in routing.

As shown in Fig. 5, Near-RT RIC has a global view of fronthaul resources and fronthaul routing in forms of the traffic matrix. Sending the whole traffic matrix to MEC for DQL can consume huge bandwidth. Near-RT RIC can use a network matrix to overcome this issue by predicting the appropriate candidate routes for fronthaul traffic. Then, Near-RT RIC sends processed fronthaul routing information to the MEC server for DQL. We consider processed fronthaul routing information to be smaller and take a short transmission time than sending the whole unprocessed traffic matrix. Since we have multiple Near-RT RICs, we use Non-RT RICs to coordinate Near-RT RICs. However, sending traffic matrix to Non-RT RIC for centralized fronthaul routing prediction may consume high bandwidth. To this end, we choose a Federated Learning (FL) approach over other approaches to learn fronthaul routing distributively. In FL, Near-RT RICs and Non-RT RIC are not required to exchange the whole traffic matrix but only the model and learning parameters. This can save bandwidth and guarantee the privacy of the fronthaul traffic matrix.

Each Near-RT RIC n can get FL model and learning parameter \mathbf{N}_t from Non-RT RIC. Then, Near-RT RIC n uses traffic matrix \mathbf{l}_n^t of size ϱ_n to improve the model through training and testing the downloaded model. We use $\mathbf{N}_t^1, \dots, \mathbf{N}_t^N$ to denote the current parameters of the ECs. Each Near-RT RIC $n \in \mathcal{N}$ computes its gradient \mathbf{N}_t^n , where \mathbf{N}_t^n is given by:

$$\mathbf{N}_t^n = \frac{1}{\varrho_n} \sum_{\varrho_n} \nabla f_{n,\varrho_n}(\mathbf{w}_n, \mathbf{l}_n^t, \tilde{\mathbf{l}}_n^t). \quad (32)$$

We use f_{n,ϱ_n} as the loss function, \mathbf{w}_n as the weight, and $\tilde{\mathbf{l}}_n^t$ as the predicted fronthaul routing at Near-RT RIC n . Furthermore, Near-RT RIC n calculates the difference Φ_t^n between its gradients \mathbf{N}_t^n and \mathbf{N}_t as follows:

$$\Phi_t^n = \mathbf{N}_t^n - \mathbf{N}_t, \forall n \in \mathcal{N}. \quad (33)$$

Each Near-RT RIC n shares Φ_t^n with Non-RT RIC. Then, Non-RT RIC aggregates the received parameters from Non-

Algorithm 1 : FL assisted DQL algorithm for joint task offloading and segment routing.

- 1: **Input:** Get communication resources and routing (from Near-RT RIC using FL), computation, and offloading states at MEC server;
- 2: **Output:** Offloading variable \mathbf{x} , fronthaul routing variable $\boldsymbol{\eta}$, computation variable \mathbf{y} , communication resources allocation \mathbf{b} , and computation resources allocation $\boldsymbol{\chi}$;
- 3: MEC server uses Target Network and Q-Network to get the Q-Values of all possible actions in the defined state;
- 4: **repeat**
- 5: Pick random action a_t or action a_t with the maximum Q-Value from the set of actions \mathcal{A} based on Υ value;
- 6: Perform action a_t , observe reward r_t and the next state s_{t+1} ;
- 7: Store $\langle s_t, s_{t+1}, a_t, r_t \rangle$ in the experience replay memory;
- 8: Sample random batches from experience replay memory and perform training of the Q-Network;
- 9: Each k th iteration, copy the weights values from the Q-Network to the Target Network;
- 10: **until** terminal state is reached
- 11: MEC server informs Near-RT RIC about updated communication resource allocation and fronthaul routing decision.

RT RICs. The parameter aggregation at Non-RT RIC is defined as follows:

$$\varphi_t = \frac{1}{N} \sum_{n=1}^N \Phi_t^n. \quad (34)$$

Furthermore, the FL update at Non-RT RIC can be expressed as follows:

$$\mathbf{N}_{t+1} = \mathbf{N}_t + \alpha \varphi_t. \quad (35)$$

Then, Non-RT RIC shares \mathbf{N}_{t+1} with Near-RT RICs. The iteration continues until $\mathbf{N}_{t+1} = \mathbf{N}_t$ (there is no more improvement of the FL model). We consider the FL model to be trained and tested once and saved for later usage to minimize the delay. Then, Near-RT RIC can load and use the pre-trained model.

A key goal of FL is to optimize a global training objective function defined over distributed devices, where each device uses its data to optimize this global training objective [38]. In our approach, we use the loss function f_{n,ϱ_n} as global training objective function, where each Near-RT RIC uses fronthaul traffic data to minimize f_{n,ϱ_n} . As discussed and proved in [38], local Stochastic Gradient Descent (SGD) with periodic averaging has $O(\frac{1}{\sqrt{NK}})$ convergence rate, where N is the number of devices, and K is the number of iterations. Therefore, our FL has $O(\frac{1}{\sqrt{NK}})$ convergence rate, where N is the number of Near-RT RICs involved in FL.

For FL assisted DQL, we propose Algorithm 1 to get offloading variable \mathbf{x} , fronthaul routing variable $\boldsymbol{\eta}$, computation variable \mathbf{y} , communication resources allocation \mathbf{b} ,

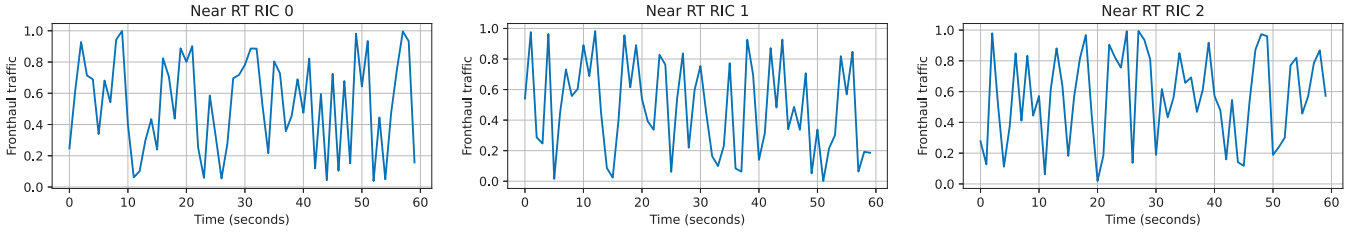


Figure 6: Normalized fronthaul traffic data at Near-RT RICs.

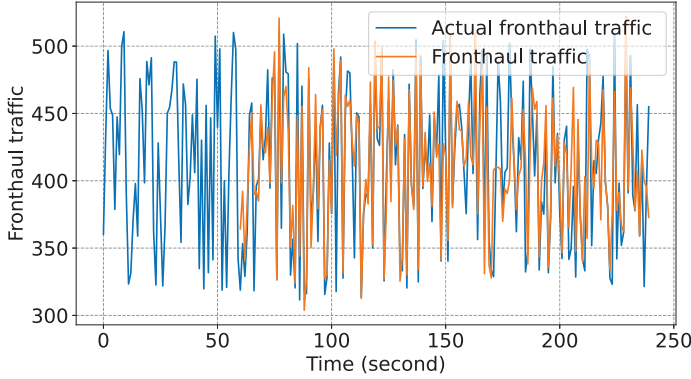


Figure 7: Prediction of fronthaul traffic (Mbps).

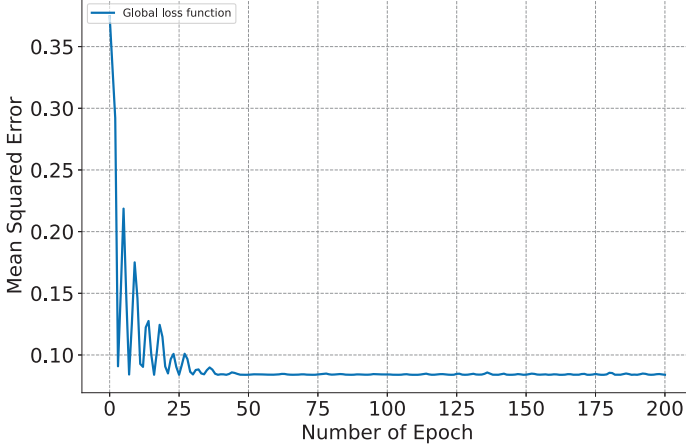


Figure 8: Convergence of global loss function f_{n, ϱ_n} .

and computation resources allocation χ . In the Algorithm 1, the MEC server gets communication resources and routing state from Near-RT RIC that uses FL, computation, and offloading states. Then, MEC server performs DQL processes. After DQL processes, the MEC server sends to Near-RT RIC updated fronthaul routing decisions. In Fig. 5, after receiving fronthaul routing decisions, Near-RT RIC sends segment paths information to the ingress TSNB to push the segment labels on the header of incoming packets. Once the segments are added to the packet header, fronthaul packets are routed through FBN using these segments.

V. PERFORMANCE EVALUATION

This section presents the performance evaluation of the proposed FL-assisted DQL for joint task offloading and fronthaul SR.

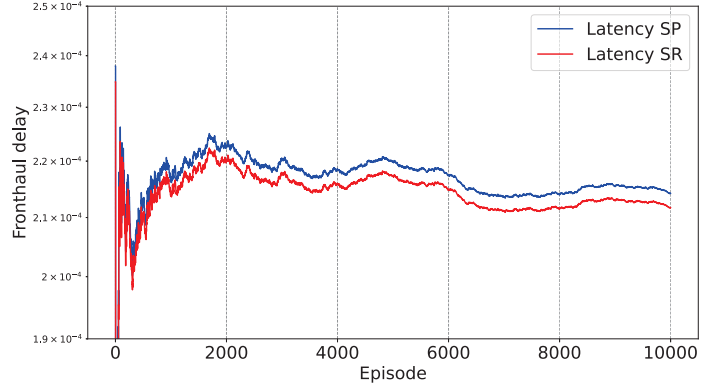


Figure 9: Delay for shortest paths vs. SR paths.

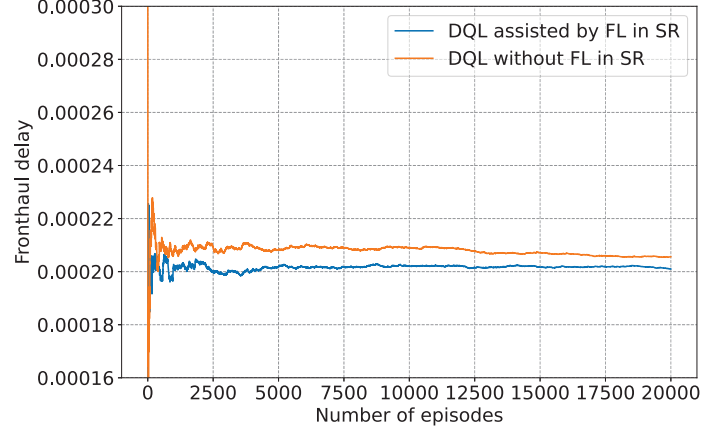


Figure 10: DQL with and without FL assistance in SR.

A. Simulation Setup

In simulation setup, we use edge devices $V = 65$, where $\tilde{z}_v = 737$ cycles per bit. For task Γ_v of the edge device, the size of the input data d_v is generated randomly within a range of 1 to 8 Mb. The task computation deadline for each device v is within a range of $\tilde{\tau}_v = 0.2$ to $\tilde{\tau}_v = 1.2$ seconds. Furthermore, each edge device has a computation resource $\chi_v = 2$ GHz. To offload the computation task in the wireless network, we set the transmission power $\rho_v = 27.0$ dBm. The channel bandwidth is in the range from $b_v^m = 25$ MHz to $b_v^m = 32$ MHz. For fronthaul routing, we use the cubical graph from NetworkX (a Python library for studying graphs and networks) [39] of 8 nodes. Each edge in graph has bandwidth in range $\omega_i^j = 6000$ to $\omega_i^j = 6500$ Mbps. The cubical graph is connected to three O-RUs and three ECs with links of bandwidth selected in the range from 6000 to 6500 Mbps. Since each EC has O-DU and

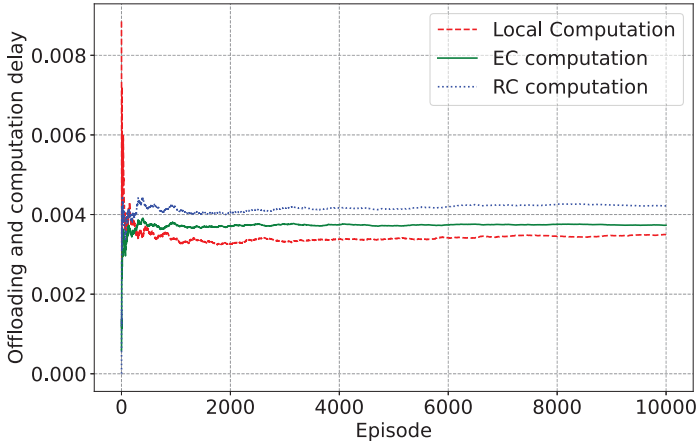


Figure 11: Offloading and computation delay.

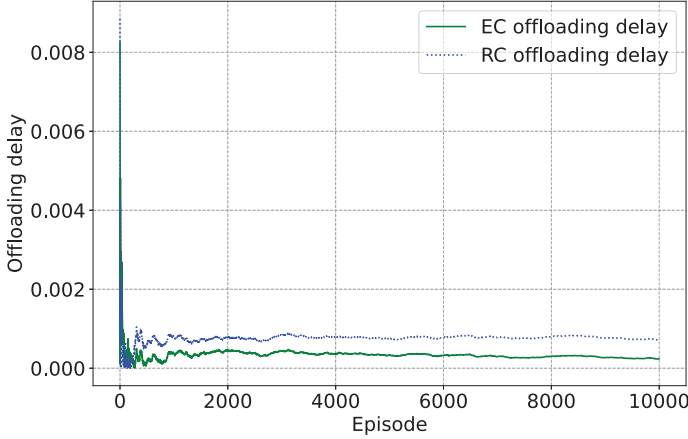


Figure 12: EC offloading vs RC offloading.

Near-RT RIC, we consider each Near-RT RIC manages one virtual fronthaul segment routing domain as overlay networks that sit on top of one fronthaul physical network. Furthermore, we consider bandwidth between each pair of ECs that hosts O-DUs in the range from $\omega_n^q = 7000$ to $\omega_n^q = 7500$ Mbps. Also, the symmetric bandwidth between each EC and RC is selected in the range from $\omega_n^{RC} = 7000$ to $\omega_n^{RC} = 7500$ Mbps. Each EC n has computation resource in the range from $\chi_n = 10$ GHz to $\chi_n = 30$ GHz, while at RC, the computation resource is in the range $\chi_{RC} = 20$ to $\chi_{RC} = 40$ GHz.

We use PyTorch [40] and Gym [41] as machine learning libraries to make Q-Network and target network for DQL. We set $\alpha = 0.001$ and $\Upsilon = 0.995$ for Q-Network and target network of 3 fully connected layers. For FL, we use TensorFlow Federated [42] and Long short-term memory (LSTM) [43] of two layers (64 neurons in the input layer and one neuron in output later) to predict fronthaul traffic in each fronthaul path. We generated a fronthaul traffic matrix using both shortest path and SR paths for 3600 seconds for FL. Based on the traffic matrix at Near-RT RICs, Fig. 6 shows the normalized fronthaul traffic at each Near-RT RIC in the range between 0 and 1. The FL model was trained offline and saved in memory, where Near-RT RIC loads the pre-trained model for predicting the fronthaul routing.

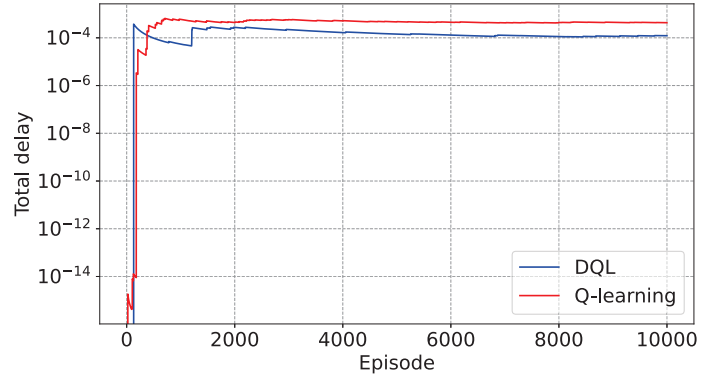


Figure 13: Total delay of DQL vs Q-Learning.

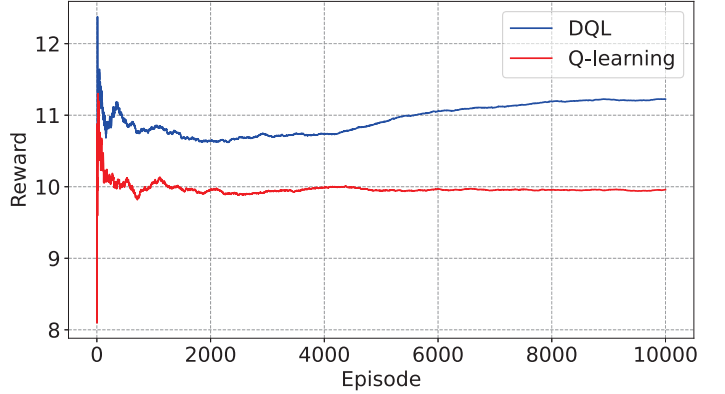


Figure 14: Maximization of reward.

B. Baseline Approaches

In the performance evaluation, for fronthaul routing, we use Dijkstra's shortest path algorithm [44] as a baseline for SP to compare with SR. SP and SR approaches use the cubical graph from NetworkX [39]. SP approach uses an unsegmented cubical graph and computes the shortest fronthaul path in the graph between source and destination. On the other hand, SR divides the cubical graph into segments, and this requires the computation of intermediate node $w \in \mathcal{W}$ that splits the fronthaul path into segments. Furthermore, for our joint task offloading, fronthaul segment routing, and edge computation problem, we consider Q-Learning and BS-MM-based solutions described in Section IV as baselines. Then, we compare DQL-based solution with Q-Learning and BS-MM-based solutions.

C. Simulation Results

Fig. 7 shows the sample of predicted fronthaul traffic at Near-RT RIC in terms of Mbps using different paths. This figure starts having predicted fronthaul traffic after 60 seconds because we use 60 seconds as a lookback period. The lookback period defines the number of time steps used to predict fronthaul traffic. In other words, using our prediction approach, we can know fronthaul traffic in 60 seconds ahead. In the initial implementation of our fronthaul routing approach for a real network environment, the Near-RT RIC should record fronthaul traffic for at least a lookback period. During this period, Near-RT RIC can use existing routing

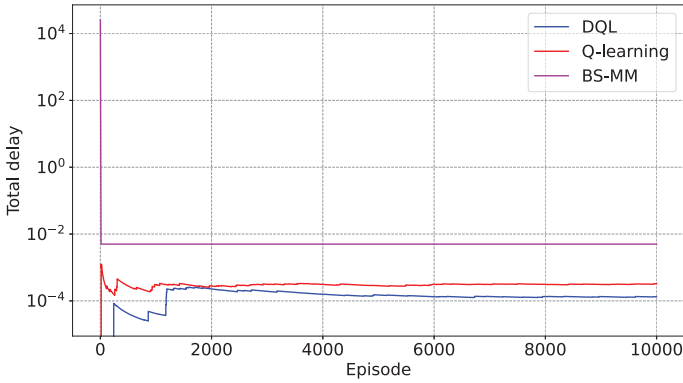


Figure 15: Total delay of BS-MM vs. DRL.

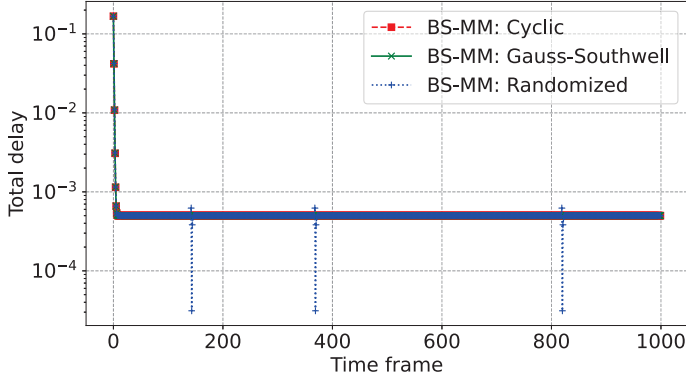


Figure 16: Delay for BS-MM in short time frame.

approaches such as Open Shortest Path First (OSPF). Then, after the lookback period, the Near-RT RIC can start using SR and select the path between SP and SR with the lowest latency to reach each egress node. Furthermore, Fig. 8 presents the convergence of MSE as global loss function f_{n, ϱ_n} , where our FL model converges starting from the 50th epoch. By using Mean Squared Error (MSE) as a loss function, our prediction reaches 0.1119 MSE.

Fig. 9 shows comparisons of fronthaul delay using all possible shorted paths and SR paths from ingress TSNBs to egress TSNBs. The results demonstrate that considering the shortest routes and the SR paths, the SR gives the lowest possible latency paths to reach egress TSNBs. After predicting the fronthaul routing and traffic, the Near-RT RIC shares routing information with MEC server for DQL (joint problem of offloading, fronthaul routing, and edge computation). Furthermore, Fig 10 shows the advantages of FL by comparing DQL with FL assistance and DQL without FL support. In DQL assisted by FL, Near-RT RIC shares predicted fronthaul routing information with MEC for DQL. In DQL without FL assistance, near-RT RIC shares fronthaul traffic matrix without using FL for prediction in SR. The simulation results show that DQL performs better when assisted by FL because decisions can be made rapidly for the lowest latency path to reach egress TSNBs. This reduces fronthaul delay.

Fig. 11 shows the total delay for computation and offloading when we compute only at edge devices, ECs, or RC. Computation at edges devices experiences lower latency

because local computation does not involve offloading delay. Also, the edge devices can minimize delay by offloading some tasks to ECs or RC. Furthermore, Fig. 12 shows offloading delay where computation delay is excluded in the results. The results from both figures (Figs 11 and 12) demonstrate that computation at RC experiences high delays because the RC is far from edge devices, which involves significant communication latency. Considering the reward function in (29), the agent needs to decide to compute locally at edge devices, offload at ECs, or RC to meet computation deadlines and avoid paying penalties. We use $\varpi_{\text{CoD}} = 0.5$, $\varpi_w = 1e-7$, $\varpi_f = 1e-4$, and $\varpi_c = 1e-10$ as penalties. Fig. 13 shows total computation delay considering all computation and offloading scenarios (at edge devices, ECs, and RC). In other words, in Fig. 13, we compared total delay related to local computation, offloading, routing, and edge computation delays using DQL and Q-learning. This figure clearly shows that using DQL has a minimum delay over Q-learning. In other words, the excellent performance of DQL is thanks to the agent/MEC server that stores previous experiences in local memory and uses neural networks' maximum output to get a new Q-Value. In Fig. 14, we compare the DQL and Q-learning in terms of reward. We run our simulation for 10000 episodes. This figure shows that DQL achieves a better performance than Q-learning in maximizing rewards (i.e., avoiding penalties for missing computation deadlines and violating resource constraints).

We compare DQL in solving (29) and optimization-based solution in solving (28). To solve (28), we use CVXPY [45] as Python library for convex optimization problems and BS-MM discussed in Section IV. Using BS-MM for long long-term optimization (considering 10000 episode corresponds to 10000 time frames) takes a long time to finish, and always DQL outperforms BS-MM and Q-learning. In Fig. 16, we compute a BS-MM-based solution in a short time frame of 1000 using Cyclic, Gauss-Southwell, and Randomized indexes selection rules [46]. BS-MM performs better for a short time frame/ short episode, but still, DQL outperforms BS-MM. Therefore, DQL can easily adopt network condition changes for a large episode than BS-MM and Q-learning.

VI. CONCLUSION

Tasks offloading from edge devices to multiple edge clouds requires wireless and fronthaul communication resources to reach edge clouds. Thus, edge clouds do not have the same available computation resources, and tasks' computation deadlines are different; we need a joint approach for task routing and distribution to multiple edge clouds. This paper proposed a new joint task offloading, segment routing for the fronthaul network, and edge computing approach in O-RAN. We formulated an optimization problem to minimize offloading, routing, and computation delay. We converted the optimization problem to the reward function. Then, we used reinforcement learning and federated learning to maximize the formulated reward by reducing the cost of delay subject to communication and computation resource constraints. The simulation results show that the proposed DQL approach outperforms Q-learning and BS-MM in

minimizing delay and increasing reward. We plan to enhance our offloading and fronthaul routing evaluation using various network scenarios and metrics as future work.

ACKNOWLEDGMENT

The authors thank Mitacs, Ciena, and ENCQOR for funding this research under the IT13947 grant.

REFERENCES

- [1] A. Ndikumana, K. K. Nguyen, and M. Cheriet, "Federated learning assisted deep q-learning for joint task offloading and fronthaul segment routing in open ran," *IEEE Transactions on Network and Service Management*, pp. 1–1, 2023.
- [2] I. Analytics, "State of the IoT 2018: Number of IoT devices now at 7B â€" market accelerating," <https://iot-analytics.com/state-of-the-iot-update-q1-q2-2018-number-of-iot-devices-now-7b/>, [Online; accessed Jan. 10, 2022].
- [3] A. Ndikumana, N. H. Tran, T. M. Ho, Z. Han, W. Saad, D. Niyato, and C. S. Hong, "Joint communication, computation, caching, and control in big data multi-access edge computing," *IEEE Transactions on Mobile Computing*, vol. 19, no. 6, pp. 1359–1374, 2019.
- [4] O. R. Alliance, "O-RAN use cases and deployment scenarios," *White Paper*, February, 2020.
- [5] O. Alliance, "O-RAN architecture description," *O-RAN-WG1-O-RAN Architecture Description - v01.00.00*, 2020.
- [6] A. Ndikumana, K. K. Nguyen, and M. Cheriet, "Age of processing-based data offloading for autonomous vehicles in multirats open ran," *IEEE Transactions on Intelligent Transportation Systems*, 2022.
- [7] I. A. Alimi, A. L. Teixeira, and P. P. Monteiro, "Toward an efficient c-ran optical fronthaul for the future networks: A tutorial on technologies, requirements, challenges, and solutions," *IEEE Communications Surveys & Tutorials*, vol. 20, no. 1, pp. 708–769, 2017.
- [8] J. Farkas, L. L. Bello, and C. Gunther, "Time-sensitive networking standards," *IEEE Communications Standards Magazine*, vol. 2, no. 2, pp. 20–21, 2018.
- [9] IEEE, "802.1CMde-2020 - IEEE standard for local and metropolitan area networks – time-sensitive networking for fronthaul," https://standards.ieee.org/standard/802_1CM-2018.html, [Online; accessed September. 30, 2020].
- [10] G. O. Pérez, D. L. Lopez, and J. A. Hernández, "5g new radio fronthaul network design for ecpri-ieee 802.1 cm and extreme latency percentiles," *IEEE Access*, vol. 7, pp. 82 218–82 230, 2019.
- [11] V. Solutions, "5G fronthaul handbook," <https://gsacom.com/paper/5g-fronthaul-handbook-viavi-solutions-dec-2019/>, Dec 2019.
- [12] V. Tong, S. Souihi, H. A. Tran, and A. Mellouk, "SDN-based application-aware segment routing for large-scale network," *IEEE Systems Journal*, 2021.
- [13] C. Carthern, W. Wilson, and N. Rivera, "Introduction to tools and automation," in *Cisco Networks*. Springer, 2021, pp. 211–217.
- [14] E. Mustafa, J. Shuja, A. I. Jehangiri, S. Din, F. Rehman, S. Mustafa, T. Maqsood, A. N. Khan *et al.*, "Joint wireless power transfer and task offloading in mobile edge computing: a survey," *Cluster Computing*, pp. 1–20, 2021.
- [15] A. Ndikumana, S. Ullah, T. LeAnh, N. H. Tran, and C. S. Hong, "Collaborative cache allocation and computation offloading in mobile edge computing," in *Proceedings of 19th Asia-Pacific Network Operations and Management Symposium (APNOMS)*. IEEE, Sep. 27-29, 2017, pp. 366–369.
- [16] A. Ndikumana, "Intelligentedge: Joint communication, computation, caching, and control in collaborative multi-access edge computing," Kyung Hee University, 2019.
- [17] A. Ndikumana and C. S. Hong, "Self-driving car meets multi-access edge computing for deep learning-based caching," in *Proceedings of 2019 International Conference on Information Networking (ICOIN)*. IEEE, Jan. 9-11, 2019 (Kuala Lumpur, Malaysia), pp. 49–54.
- [18] Z. Wu, K. Wang, H. Ji, and V. C. Leung, "A computing offloading algorithm for f-ran with limited capacity fronthaul," in *2016 IEEE International Conference on Network Infrastructure and Digital Content (IC-NIDC)*. IEEE, 2016, pp. 78–83.
- [19] K. Kaneva, N. Aboutorab, and G. Leu, "Multi-hop fronthaul offloading in learning-aided fog computing," in *2021 IEEE 93rd Vehicular Technology Conference (VTC2021-Spring)*. IEEE, 2021, pp. 1–7.
- [20] Y. Nakayama, D. Hisano, T. Kubo, Y. Fukada, J. Terada, and A. Otaka, "Low-latency routing scheme for a fronthaul bridged network," *Journal of Optical Communications and Networking*, vol. 10, no. 1, pp. 14–23, 2018.
- [21] J. Park, S. Samarakoon, A. Elgabli, J. Kim, M. Bennis, S.-L. Kim, and M. Debbah, "Communication-efficient and distributed learning over wireless networks: Principles and applications," *arXiv preprint arXiv:2008.02608*, 2020.
- [22] T. Li, A. K. Sahu, A. Talwalkar, and V. Smith, "Federated learning: Challenges, methods, and future directions," *IEEE Signal Processing Magazine*, vol. 37, no. 3, pp. 50–60, 2020.
- [23] K. Xiong, S. Leng, C. Huang, C. Yuen, and L. Guan, "Intelligent task offloading for heterogeneous v2x communications," *arXiv preprint arXiv:2006.15855*, Jun 29, 2020.
- [24] J. Chen, S. Chen, S. Luo, Q. Wang, B. Cao, and X. Li, "An intelligent task offloading algorithm (itof) for uav edge computing network," *Digital Communications and Networks*, 2020.
- [25] X. Chen, C. Wu, Z. Liu, N. Zhang, and Y. Ji, "Computation offloading in beyond 5G networks: A distributed learning framework and applications," *arXiv preprint arXiv:2007.08001*, 15 Jul. 2020.
- [26] S. Rantakokko, "Data handling process in extended reality (XR) when delivering technical instructions," *Technical Communication*, vol. 69, no. 2, pp. 75–96, 2022.
- [27] T. N. Nguyen and S. Zeadally, "Mobile crowd-sensing applications: Data redundancies, challenges, and solutions," *ACM Transactions on Internet Technology (TOIT)*, vol. 22, no. 2, pp. 1–15, 2021.
- [28] Y. Huang, X. Xu, N. Li, H. Ding, and X. Tang, "Prospect of 5g intelligent networks," *IEEE Wireless Communications*, vol. 27, no. 4, pp. 4–5, 2020.
- [29] Y. Zhou, F. R. Yu, J. Chen, and Y. Kuo, "Resource allocation for information-centric virtualized heterogeneous networks with in-network caching and mobile edge computing," *IEEE Transactions on Vehicular Technology*, vol. 66, no. 12, pp. 11 339–11 351, 2017.
- [30] F. Hao, M. Kodialam, and T. Lakshman, "Optimizing restoration with segment routing," in *IEEE INFOCOM 2016-The 35th Annual IEEE International Conference on Computer Communications*. IEEE, 2016, pp. 1–9.
- [31] G. Trimponias, Y. Xiao, H. Xu, X. Wu, and Y. Geng, "Centrality-based middlepoint selection for traffic engineering with segment routing," *arXiv preprint arXiv:1703.05907*, 2017.
- [32] Y. K. Tun, S. R. Pandey, M. Alsenwi, C. W. Zaw, and C. S. Hong, "Weighted proportional allocation based power allocation in wireless network virtualization for future wireless networks," in *2019 International Conference on Information Networking (ICOIN)*. IEEE, 2019, pp. 284–289.
- [33] Y. Sun, P. Babu, and D. P. Palomar, "Majorization-minimization algorithms in signal processing, communications, and machine learning," *IEEE Transactions on Signal Processing*, vol. 65, no. 3, pp. 794–816, 2016.
- [34] A. Ndikumana, N. H. Tran, K. T. Kim, C. S. Hong *et al.*, "Deep learning based caching for self-driving cars in multi-access edge computing," *IEEE Transactions on Intelligent Transportation Systems*, Mar 4, 2020.
- [35] R. S. Sutton and A. G. Barto, *Reinforcement learning: An introduction*. MIT press, 2018.
- [36] E. A. Feinberg and A. Shwartz, *Handbook of Markov decision processes: methods and applications*. Springer Science & Business Media, 2012, vol. 40.
- [37] J. Fan, Z. Wang, Y. Xie, and Z. Yang, "A theoretical analysis of deep q-learning," in *Learning for Dynamics and Control*. PMLR, 2020, pp. 486–489.
- [38] F. Haddadpour and M. Mahdavi, "On the convergence of local descent methods in federated learning," *arXiv preprint arXiv:1910.14425*, 2019.
- [39] NetworkX, "NetworkX: Network analysis with python," <https://networkx.org/>, [Online; accessed Nov. 22, 2021].
- [40] A. Paszke, S. Gross, F. Massa, A. Lerer, J. Bradbury, G. Chanan, T. Killeen, Z. Lin, N. Gimelshein, L. Antiga *et al.*, "Pytorch: An imperative style, high-performance deep learning library," *Advances in neural information processing systems*, vol. 32, pp. 8026–8037, 2019.

- [41] G. Brockman, V. Cheung, L. Pettersson, J. Schneider, J. Schulman, J. Tang, and W. Zaremba, "Openai gym," *arXiv preprint arXiv:1606.01540*, 2016.
- [42] TensorFlow, "TensorFlow Federated: Machine learning on decentralized data," <https://www.tensorflow.org/federated>, [Online; accessed September. 30, 2020].
- [43] M. Z. Alom, T. M. Taha, C. Yakopcic, S. Westberg, P. Sidike, M. S. Nasrin, B. C. Van Esesn, A. A. S. Awwal, and V. K. Asari, "The history began from alexnet: A comprehensive survey on deep learning approaches," *arXiv preprint arXiv:1803.01164*, 2018.
- [44] H. Wei, S. Zhang, and X. He, "Shortest path algorithm in dynamic restricted area based on unidirectional road network model," *Sensors*, vol. 21, no. 1, p. 203, 2021.
- [45] S. Diamond and S. Boyd, "CVXPY: A Python-embedded modeling language for convex optimization," *Journal of Machine Learning Research*, vol. 17, no. 83, pp. 1–5, 2016.
- [46] A. Ndikumana, N. H. Tran, T. M. Ho, D. Niyato, Z. Han, and C. S. Hong, "Joint incentive mechanism for paid content caching and price based cache replacement policy in named data networking," *IEEE Access*, vol. 6, pp. 33 702–33 717, 2018.



Anselme Ndikumana received B.S. degree in Computer Science from the National University of Rwanda in 2007 and Ph.D. degree in Computer Engineering from Kyung Hee University, South Korea in August 2019. Since 2020, he has been with the Synchronmedia Lab, École de Technologie Supérieure, Université du Québec, Montréal, QC, Canada, where he is currently a Postdoctoral Researcher. His professional experience includes Lecturer at the University of Lay Adventists of Kigali from 2019

to 2020, Chief Information System, a System Analyst, and a Database Administrator at Rwanda Utilities Regulatory Authority from 2008 to 2014. His research interest includes AI for wireless communication, multi-access edge computing, 5G and next-G networks, metaverse, network economics, game theory, and network optimization.



Kim Khoa Nguyen is Associate Professor in the Department of Electrical Engineering and the founder of the Laboratory on IoT and Cloud Computing at the University of Quebec's Ecole de technologie supérieure. In the past, he served as CTO of Inocybe Technologies (now is Kontron Canada), a world's leading company in software-defined networking (SDN) solutions. He was the architect of the Canarie's GreenStar Network and led R&D in large-scale projects with Ericsson, Ciena, Telus, InterDigital, and

Ultra Electronics. He is the recipient of Microsoft Azure Global IoT Contest Award 2017, and Ciena's Aspirational Prize 2018. He is the author of more than 100 publications, and holds several industrial patents. His expertise includes network optimization, cloud computing IoT, 5G, big data, machine learning, smart city, and high speed networks.



Dr. Mohamed Cheriet received his Bachelor, M.Sc. and Ph.D. degrees in Computer Science from USTHB (Algiers) and the University of Pierre & Marie Curie (Paris VI) in 1984, 1985 and 1988 respectively. He was then a Postdoctoral Fellow at CNRS, Pont et Chaussées, Paris V, in 1988, and at CENPARMI, Concordia U., Montreal, in 1990. Since 1992, he has been a professor in the Systems Engineering department at the University of Quebec - École de Technologie Supérieure (ÉTS), Montreal, and was appointed

full Professor there in 1998. Prof. Cheriet was the director of LIVIA Laboratory for Imagery, Vision, and Artificial Intelligence (2000-2006), and is the founder and director of Synchronmedia Laboratory for multimedia communication in telepresence applications, since 1998. Dr. Cheriet research has extensive experience in Sustainable and Intelligent Next Generation Systems. Dr. Cheriet is an expert in Computational Intelligence, Pattern Recognition, Machine Learning, Artificial Intelligence and Perception and their applications, more extensively in Networking and Image Processing. In addition, Dr. Cheriet has published more than 500 technical papers in the field and serves on the editorial boards of several renowned journals and international conferences. He held a Tier 1 Canada Research Chair on Sustainable and Smart Eco-Cloud (2013-2000), and lead the establishment of the first smart university campus in Canada, created as a hub for innovation and productivity at Montreal. Dr. Cheriet is the General Director of the FRQNT Strategic Cluster on the Operationalization of Sustainability Development, CIRODD (2019-2026). He is the Administrative Director of the \$12M CFI'2022 CEOS*Net Manufacturing Cloud Network. He is a 2016 Fellow of the International Association of Pattern Recognition (IAPR), a 2017 Fellow of the Canadian Academy of Engineering (CAE), a 2018 Fellow of the Engineering Institute of Canada (EIC), and a 2019 Fellow of Engineers Canada (EC). Dr. Cheriet is the recipient of the 2016 IEEE J.M. Ham Outstanding Engineering Educator Award, the 2013 ÉTS Research Excellence prize, for his outstanding contribution in green ICT, cloud computing, and big data analytics research areas, and the 2012 Queen Elizabeth II Diamond Jubilee Medal. He is a senior member of the IEEE, the founder and former Chair of the IEEE Montreal Chapter of Computational Intelligent Systems (CIS), a Steering Committee Member of the IEEE Sustainable ICT Initiative, and the Chair of ICT Emissions Working Group. He contributed 6 patents (3 granted), and the first standard ever, IEEE 1922.2, on real-time calculation of ICT emissions, in April 2020, with his IEEE Emissions Working Group.